Validation of Computational Fluid Dynamics Methods with Anatomically Exact, 3D Printed MRI Phantoms and 4D pcMRI

Jeff R. Anderson, Orlando Diaz, Richard Klucznik, Y. Jonathan Zhang, Gavin W. Britz, Robert G. Grossman, Nan Lv, Qinghai Huang, Christof Karmonik

Abstract— **A new concept of rapid 3D prototyping was implemented using cost-effective 3D printing for creating anatomically correct replica of cerebral aneurysms. With a dedicated flow loop set-up in a full body human MRI scanner, flow measurements were performed using 4D phase contrast magnetic resonance imaging to visualize and quantify intra-aneurysmal flow patterns. Ultrashort TE sequences were employed to obtain high-resolution 3D image data to visualize the lumen inside the plastic replica. In-vitro results were compared with retrospectively obtained in-vivo data and results from computational fluid dynamics simulations (CFD). Rapid prototyping of anatomically realistic 3D models may have future impact in treatment planning, design of image acquisition methods for MRI and angiographic systems and for the design and testing of advanced image post-processing technologies.**

INTRODUCTION

Simulating the hemodynamics incident to cerebral aneurysms with computational fluid dynamics (CFD) is a relatively new and promising field [1, 2]. The essence of the method consists in modeling real world hemodynamics with a computational approximation. Mathematical models vary but generally address factors such as geometrical approximations, boundary conditions, inflow waveforms, and governing blood flow equations (Navier Stokes equations). The output of such computations is a 3D velocity field and other related parameters derived from it such as wall shear stress and pressure. An important aspect towards the acceptance of computational simulations is their validation by direct comparison with measurements [3, 4]. A variety of non-invasive methods exist to obtain information about intracranial blood velocity measurements, such as ultrasound Doppler velocity, optical flow analysis of projections angiographic X-ray images or 2D and 4D phase contrast magnetic resonance imaging (pcMRI [3-6, 7]) . The latter has been previously demonstrated in selected studies to visualize and quantify major intra-aneurysmal flow patterns and yielded good agreement with CFD results [8-10]. While pcMRI methods hold great potential for measuring intra-aneurysmal flow, their optimization in-vivo with the actual patient is limited. MRI examinations are not part of the standard clinical workup in this patient group and the duration of an MRI examination for research purposes only has to be limited in order to reduce discomfort to the patient and to minimize the risk of an adverse event (such as aneurysm rupture). An alternative is the use of an anatomically exact phantom which can be used in the MRI scanner. Recent advances of 3D rapid prototyping technology now allow one to quickly and cost-effectively create an accurate 3D representation of anatomy. Here, we explore a 3D printing technology for creating flow phantoms based on medical image data of cerebral aneurysm for use with a flow loop within a clinical MRI scanner.

J. R. Anderson is with the Department of Translational Imaging, Houston Methodist Research Institute, Houston, TX 77030 USA (phone: 713-441-3800; fax: 771-441-0845).

O. Diaz and R. Klucznik are with the Department of Radiology Houston Methodist Research Institute, Houston, TX 77030 USA

Y. J. Zhang, G. W. Britz, R. G. Grossman and C. Karmonik are with the Department of Neurosurgery Houston Methodist Research Institute, Houston, TX 77030 USA.

N. Lv and Q. Huang are with the Affiliated Changhai Hospital of Second Military Medical University, Shanghai, China

I. METHODS

A. 3D Printing Models

From 3D digital subtraction angiography (Siemens AX, 3D DSA) images acquired during diagnostic angiographic procedures, 3D models of 6 cerebral aneurysms were created and stored as stereolithographic (STL) files. Approval of this retrospective study was obtained by the institutional review board. STL files were loaded into netfabb Basic, version 5.1 (Netfabb GmbH, Eichenbuehl, Germany) and an automatic repair of the STL surface file was performed to ensure the elimination of holes.

B. 3D Printing

Repaired STL files were loaded into Makerware version 2.4.1 (Makerbot, New York, NY, USA) and anatomical correctly sized 3D printouts were created with the following parameters: infill: zero percent, number of shells: 2, and layer height: 0.2 mm on a Makerbot Replicator, 2nd generation 3D printer. PLA (polylactide resin) filaments were used in the printing process (NatureWorks LLC, Minnetonka MN, USA).

C. Flow Loop

A closed flow loop was constructed to supply flow with physiologically realistic velocities (up to 100 cm/sec). The flow pump was located outside of the scanner room and connected through waveguides to the aneurysm phantom which was placed into the wrist coil of a 3T whole-body MRI scanner (Ingenia, Philips, Magnetic Resonance Imaging facility of the Houston Methodist Research Institute, http://www.houstonmethodist.org/mri-core). Water doped with a Gd-based MRI contrast agent was used.

D. MRI Protocol

The MRI protocol consisted of three different kinds of acquisitions. After scout scanning, a T1-weighted, high resolution spin echo scan was acquired to obtain detailed information about the orientation of the aneurysm. Imaging parameters were as follows: TR = 1995 ms, TE = 9.3 ms,

978-1-4244-7929-0/14/$26.00 ©2014 IEEE

voxel resolution = 0.5 mm isotropic, imaging matrix = 128 × 128, number of slices = 128. Then, a 4D pcMRI acquisition was performed which yielded a true 3D representation of the velocity field within the aneurysm. Imaging parameters were as follows: TR = 10 ms, TE = 5.9 ms, flip angle = 15°, voxel resolution = 1.0 mm isotropic, imaging matrix = 64 × 64 × 64, PC velocity = 110 cm/s. Last, a 3D, radially acquired ultrashort TE (UTE) image was obtained to obtain a better visualization of the plastic phantom than available by standard imaging sequences. Imaging parameters were as follows: TR = 11 ms, TE = 0.15 ms, flip angle = 8°, voxel resolution = 0.5 mm isotropic, imaging matrix = 128 × 128 × 128.

E. Image Post-Processing

MRI images were transferred to a dedicated workstation for postprocessing (Apple, Mac Pro, Quad core) using ImageJ (NIH, Bethesda, USA) and paraview (Kitware, Inc, Clifton Park, NY, USA). First, phase difference images from the 4D pcMRI acquisition were masked by the magnitude images to eliminate contamination of the image data by the phase value artifacts; anything but the aneurysm lumen. Gray scale values of the phase difference images were scaled as follows:

$$S^* = \frac{(S_0 - S_{stat})}{R/2} \times VENC$$

with S_0: measured gray scale intensity, S_{stat}: intensity of stationary tissue (2048), R: intensity range (4096) and VENC: velocity encoding coefficient (110 cm/sec).

Then, a 3D contour was created in paraview based on the magnitude images. Velocity vectors were constructed from the gray scale values of the differently encoded velocity directions as follows:

$$v = RL \times i + AP \times j + FH \times k$$

with RL corresponding to the image gray scale value for velocity encoding in the right-left direction, AP in the anterior-posterior direction, and FH in the foot-head direction and with i, j, and k being the unit vectors of the Cartesian space.

F. Comparison with In-vivo and CFD

For aneurysm model 3, *in vivo* acquired 2D pcMRI data (Avanto, 1.5T, Siemens MR) as well as results from CFD simulations were available from a previous study . [11] These data were compared with those obtained here with the flow loop.

II. Results

A. 3D Printing

Depending on the size of the aneurysm model, the printing process lasted from 20 min to one hour (figure 1). Models were printed with closed inlets and outlets and and with support struts. These were removed manually following printing. One printout initially failed due to insufficient strut support. However, orienting the build in a slightly oblique to the first, the model printed without error.

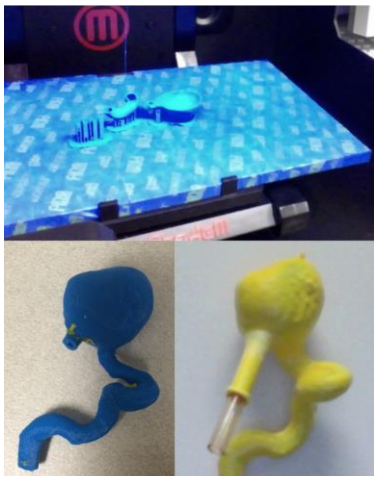

Figure 1. The Printing process. An aneurysm phantom is shown mid-print (top), fully printed (bottom left), and ready for imaging (bottom right).

B. 4D pcMRI Images

In all aneurysm models, major intra-aneurysm flow patterns were easily discernible (figure 2) by regions of bright (flow perpendicular to the view plane towards the viewer) and dark (flow perpendicular to the view plane away from the viewer). In all aneurysms, a circular motion of flow was apparent in the aneurysm by alternating of bright and dark regions in the slices intersecting the aneurysm dome. Quantification of flow in the parent artery segment proximal to the aneurysm ostium yielded velocity measurements representing inflow into the aneurysm model.

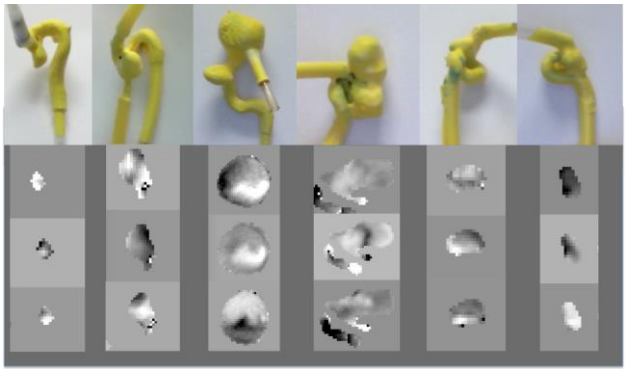

Figure 2. Photos of all six aneurysm phantoms are shown along with corresponding flow images for each. The images are taken in the AP (top), FH (middle), and RL (bottom) directions. Only a single "slice" from the 3D volume of data is shown.

C. 3D Flow Pattern

Reconstructing flow streamlines with paraview succeeded in all cases thereby visualizing the well familiar vortex flow pattern within the aneurysm dome (figure 3).

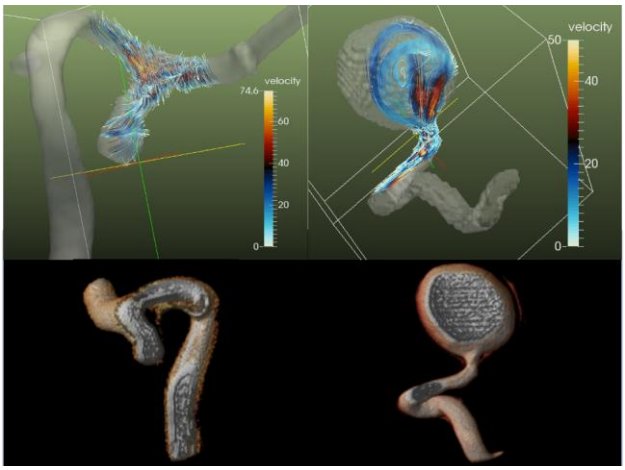

Figure 3. Two representative flow streamline visualizations are shown (aneurysm 1, left, and aneurysm 3, right). 3D visualizations from UTE images are shown as well (bottom). The UTE images are able to distinguish liquids inside the phantoms (white tones) from the printed material of the phantom (red tones).

D. Comparison with In-vivo and CFD

In the one aneurysm model, where in-vivo 2D pcMRI and CFD data was available, the inflow into the aneurysm dome consisted in-vivo of a prominent inflow jet with a perpendicular crescent cross section. This cross section, which was previously reported to be well matched by CFD simulations, was also reproduced by the in-vitro results reported here (figure 4) encouraging further application and refinement of the approach described here.

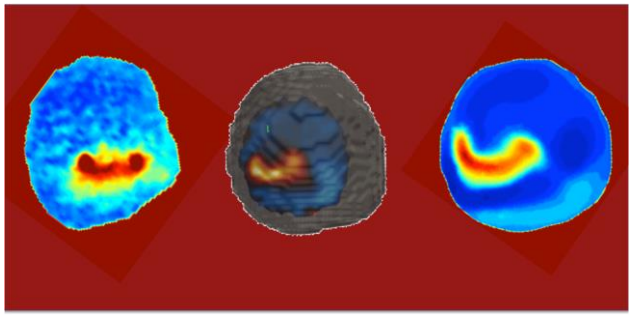

Figure 4. This figure highlights the pominent inflow jet seen in aneurysm 3. The image on the left is from in-vivo measurement, the image in the center from in-vitro phantom measurement, and the image on the right from in-silico CFD simulations. All images were manually co-oriented with each other.

III. Discussion

Flow measurements in models of cerebral aneurysm and a comparison of results with CFD simulations have been reported previously [3, 4]. Here we describe a fast and inexpensive method of creating accurate 3D anatomical models from medical images with already established technologies. Export of STL files has previously been pioneered particularly for obtaining virtual 3D surface models for use in CFD simulations [11]. The Makerbot family provides a cost-effective and - as we found - very reliable and fast approach to obtain 3D printouts. While one application of the in-vitro models consist in the validation of computational simulations, other applications could result in pre-treatment planning for endovascular procedures, sizing of medical devices (stent or flow diverter lengths), optimization of image acquisition procedures and validation of new image analysis methods. The advantage of having a realistic 3D model available within a couple of hours may even be of advantage in treatment planning for the individual patient.

IV. Conclusion

A new concept of rapid prototyping for the creation of anatomically correct replica of cerebral aneurysms is presented and applied for the visualization and quantification of intra-aneurysmal velocity patterns using 4D phase contrast magnetic resonance imaging. First comparison with CFD and in-vivo measurements are encouraging warranting further application of the here presented technique. Future work also includes implementing pulsatile flow and incorporating flexible walled phantoms.

References

[1] C. M. Strother and J. Jiang, "Intracranial aneurysms, cancer, x-rays, and computational fluid dynamics," *AJNR Am J Neuroradiol,* vol. 33, pp. 991-2, Jun.

[2] J. R. Cebral and H. Meng, "Counterpoint: realizing the clinical utility of computational fluid dynamics--closing the gap," *AJNR Am J Neuroradiol,* vol. 33, pp. 396-8, Mar.

[3] Q. Sun, A. Groth, and T. Aach, "Comprehensive validation of computational fluid dynamics simulations of in-vivo blood flow in patient-specific cerebral aneurysms," *Med Phys,* vol. 39, pp. 742-54, Feb.

[4] Q. Sun, A. Groth, M. Bertram, I. Waechter, T. Bruijns, R. Hermans, and T. Aach, "Phantom-based experimental validation of computational fluid dynamics simulations on cerebral aneurysms," *Med Phys,* vol. 37, pp. 5054-65, Sep.

[5] J. Endres, M. Kowarschik, T. Redel, P. Sharma, V. Mihalef, J. Hornegger, and A. Dorfler, "A workflow for patient-individualized virtual angiogram generation based on CFD simulation," *Comput Math Methods Med,* vol. 2012, p. 306765.

[6] C. Monninghoff, S. Maderwald, J. M. Theysohn, O. Kraff, S. C. Ladd, M. E. Ladd, M. Forsting, H. H. Quick, and I. Wanke, "Evaluation of intracranial aneurysms with 7 T versus 1.5 T time-of-flight MR angiography - initial experience," *Rofo,* vol. 181, pp. 16-23, Jan 2009.

[7] J. Jiang, K. Johnson, K. Valen-Sendstad, K. A. Mardal, O. Wieben, and C. Strother, "Flow characteristics in a canine aneurysm model: a comparison of 4D accelerated phase-contrast MR measurements and computational fluid dynamics simulations," *Med Phys,* vol. 38, pp. 6300-12, Nov.

[8] C. Karmonik, O. Diaz, R. Grossman, and R. Klucznik, "In-Vivo Quantification of Wall Motion in Cerebral Aneurysms from 2D Cine Phase Contrast Magnetic Resonance Images," *Rofo,* Oct 26 2009.

[9] C. Karmonik, R. Klucznik, and G. Benndorf, "Comparison of velocity patterns in an AComA aneurysm measured with 2D phase contrast MRI and simulated with CFD," *Technol Health Care,* vol. 16, pp. 119-28, 2008.

[10] C. Karmonik, C. Yen, E. Gabriel, S. Partovi, M. Horner, Y. J. Zhang, R. P. Klucznik, O. Diaz, and R. G. Grossman, "Quantification of speed-up and accuracy of multi-CPU computational flow dynamics simulations of hemodynamics in a posterior communicating artery aneurysm of complex geometry," *J Neurointerv Surg,* vol. 5 Suppl 3, pp. iii48-55, Nov.

[11] C. Karmonik, R. Klucznik, and G. Benndorf, "Blood flow in cerebral aneurysms: comparison of phase contrast magnetic resonance and computational fluid dynamics--preliminary experience," *Rofo,* vol. 180, pp. 209-15, Mar 2008.